

## Individual-based model with global competition interaction: Fluctuation effects in pattern formation

E. Brigatti,<sup>1,\*</sup> V. Schwämmle,<sup>2</sup> and Minos A. Neto<sup>1</sup><sup>1</sup>*Instituto de Física, Universidade Federal Fluminense, Campus da Praia Vermelha, 24210-340 Niterói, Rio de Janeiro, Brazil*<sup>2</sup>*Centro Brasileiro de Pesquisas Físicas, Rua Dr. Xavier Sigaud 150, 22290-180 Rio de Janeiro, Rio de Janeiro, Brazil*

(Received 7 March 2007; revised manuscript received 16 November 2007; published 26 February 2008)

We present some numerical results obtained from a simple individual-based model that describes clustering of organisms caused by competition. Our aim is to show that, even when a deterministic description developed for continuum models predicts no pattern formation, an individual-based model displays well-defined patterns, as a consequence of fluctuation effects caused by the discrete nature of the interacting agents.

DOI: [10.1103/PhysRevE.77.021914](https://doi.org/10.1103/PhysRevE.77.021914)

PACS number(s): 87.17.Aa, 87.23.Kg, 05.10.Ln

### I. INTRODUCTION

Birth and death processes are two of the most relevant characteristics of the dynamics of biological populations and can be responsible for the emergence of stable spatial patterns [1]. In fact, the intrinsic asymmetry in the nature of birth and death processes can enhance small initial differences in the spatial population density and lead to the formation of structures [2–4]. These clusters are resistant to some levels of diffusion and emerge as soon as the birth of new individuals outcompetes their movements. For this reason, simplified models combining birth and death processes with Brownian movement are able to describe aggregation of individuals [5].

Another central ingredient, present in ecological systems, that can cause the generation of spatial structures is the competition for resources [6–8]. Different individuals struggle for nutrients with a competition strength directly dependent on the individuals' spatial density within the competing range. Reproduction and/or death rates depending on the number of individuals in the surroundings can represent this kind of interaction. This feature has attracted the interest of experts from a variety of fields, ranging from pure mathematics [9] and nonlinear physics [10–15] to population biology [16,17] and theoretical studies in evolutionary theory [18–23]. In addition, similar behaviors can be found in physical systems, such as, for example, in mode interaction in crystallization fronts [24] and in spin-wave patterns [25]. It is remarkable that the structured state generated by this kind of frequency-dependent interaction exists only for some specific form of the interaction [22] and is reached through a transition in the parameter space. This transition (*segregation transition* [10]) drives the steady state of the system from a spatially homogeneous distribution to one marked by some clearly distinguishable inhomogeneities.

All these models, characterized by diffusion effects and an implementation of frequency-dependent birth and death processes, permit multiple interpretations.

In a common interpretation the system space directly represents the physical space where the organisms live and the diffusion represents their spatial movement. Competition be-

tween individuals corresponds to a mechanism of growth control caused by limited common resources. In this case, pattern formation can reproduce the evolution of bacterial colonies [6], plankton concentration [5], development of vegetation [8], or spatial distribution of predators [7].

On the other hand, a different interpretation enables us to describe the speciation process: the generation of two different species starting from one single continuous population of interbreeding organisms. To be specific, we can describe the speciation process by representing all the phenotypic characteristics that determine the biological success of an individual by a number, the strategy value, that labels each individual. By reproduction, which includes a mutation process, an offspring inherits a strategy that slightly differs from that of its parent. In order to model natural selection, a frequency-dependent mechanism that mimics competition completes the ingredients necessary for the emergence of population clustering. In this scenario, the generation of a new cluster is interpreted, in a broad sense, as a speciation event. Now, if the model space represents the mentioned strategy space and the diffusion models the mutation process during reproduction, we can identify the mechanism of growth control with natural selection and the branching events with the speciation process. This different interpretation justifies the analogy between a model that describes the speciation process and the ones that describe spatial pattern formation in the evolution of bacterial colonies, vegetation, or predation.

We must remember that, since this model does not include sexual reproduction, we are describing trait divergence in an asexual population, rather than speciation. Anyway, apart from effects strictly related to sexual reproduction, the dynamics characterized by the individuals' diffusion from regions of low viability in favor of more viable ones is the essential core of these two phenomena. A detailed and motivated discussion of these processes can be found in Refs. [18–23].

We can describe such processes starting from an individual-based model, which yields information on the behavior of a finite system (finite population) and accounts for fluctuation effects caused by the discrete nature of the interacting agents. Another approach, that neglects fluctuations, describes individuals just with the use of a field that represents the population density at each position in space over time. This method, usually called the continuous mean-field

\*edgardo@if.uff.br

description [15,26], becomes exact in the infinite-size limit if fluctuations are small compared to averages [4]. Note that we are not making a mean-field approximation in the nature of the interaction (see, for instance, Ref. [27]), which, in our model, is local and different for each individual.

Choosing this second strategy, the generalization of a well-investigated equation (Fisher-Kolmogoroff-Petrovsky-Piscounoff [28]) is quite common at present. In addition to a diffusion process with coefficient  $D$  and a population growth mechanism (rate  $a$ ), this equation incorporates a growth-limiting process controlled by the parameter  $b$  [11,12,14]:

$$\frac{\partial \rho(x,t)}{\partial t} = D \nabla^2 \rho(x,t) + a \rho(x,t) - b \rho(x,t) \int_{-\infty}^{+\infty} \rho(y,t) F(x,y) dy, \quad (1)$$

where  $\rho$  is the density of individuals at position  $x$  and time  $t$ . Competition is obtained by varying the death probability for each individual, and is controlled through the *influence function*  $F(x,y)$ . Let us focus on the shape of the influence function: it can range from a simple boxlike function to a globally uniform interaction. However, the Gaussian function should be considered particularly relevant. If, for instance, we need to represent the activity of a sedentary animal, the interaction represented in the influence function should take into account the individual's daily excursion around the fixed breeding site, which can be represented by Brownian motion and, for this reason, by a Gaussian distribution. In the same way, if we want to represent the habitat degeneration induced by the growth of a colony of plants [29], we can think that the colony is originated by a single individual that disperses its seeds in a way also well described by Brownian motion. More generally, for a biological interaction that does not stop at some defined length (presence of a cutoff), and that is nonlocal and controlled by a purely stochastic process, the Gaussian function should be the most natural choice. On the other hand, this choice is a source of complications. Deterministic descriptions, in the case of a Gaussian influence function, predict no pattern formation [12,30]. However, such descriptions do not take into account fluctuations arising from the discrete character of individuals. The importance of these fluctuations has been recently pointed out in a quite paradigmatic example, where random-walking organisms that reproduce and die at a constant rate spontaneously aggregate [2–5,31].

The deterministic approximation is not able to show this behavior, and is incapable of capturing the essential asymmetry between birth, a multiplicative process that increments the density in the regions adjacent to the parent, and death events, which occur anywhere. Even when the patterns can be obtained within the deterministic description, a recent work outlines the importance of fluctuations by showing their impact on transition points and amplitudes [14,32,33].

In this work, we present some numerical results obtained by means of a simple individual-based model. Our aim is to show the appearance of a segregation transition in a model where the deterministic instability, produced by the nonlocal interaction, is not sufficient for generating inhomogeneities [12], but the superimposed microscopic stochastic fluctua-

tions permit the emergence of patterns. Moreover, we compare the model implementation in the strategy space with the implementation in the physical space. In the first, used to characterize the speciation process, diffusion corresponds to a mutation phenomenon, operating just one time in each individual's life. In the second, directly related to the reaction-diffusion equation [Eq. (1)], diffusion describes a typical Brownian motion.

The paper is organized as follows. The next section describes the model used in our simulations. Section III shows, for specific values of the parameters, the emergence of spatially inhomogeneous steady states. In Sec. IV we prove that these patterns are not caused by some finite-size effect. Section V is devoted to illustrate the segregation transition and general conditions that allow spatial segregation of arbitrary wavelengths. In Sec. VI we describe, in the light of the existing literature, the cluster size dependence on diffusion rate and population size and give some hints related to the behavior of fluctuations. Conclusions are reported in Sec. VII.

## II. THE MODEL

The simulations start with an initial population of  $N_0$  individuals located along a ring of length  $L$ , i.e., we take periodic boundary conditions. At each time step, our model is controlled by the following microscopic rules.

(1) Each individual, characterized by its position  $x$ , dies with probability  $P$ ,

$$P = K \sum_{j=1}^{N(\tau)} \exp\left(-\frac{(x-y_j)^2}{2C^2}\right), \quad (2)$$

where  $N(\tau)$  is the total number of individuals at the actual step  $\tau$  and  $y_j$  is the respective individuals' positions. The distance between two individuals is obtained by taking the shorter distance on the ring. The strength of competition declines with increasing distance according to a Gaussian function with deviation  $C$ . The parameter  $K$  depicts the carrying capacity.

(2) If the individual survives this death selection, it reproduces. The newborn, starting from the parent's location, moves in a random direction a distance obtained from a Gaussian distribution of standard deviation  $\sigma$ . This change represents the effect of mutations in the offspring phenotype.

As soon as all the individuals have passed the death selection and eventually reproduced, the next time step begins. This model implementation is analogous to the diffusion process described by Eq. (1).

To establish a more direct comparison between that mean-field description and the individual-based simulation, we have also implemented the model with an exact microscopic representation of the diffusion term. In this case, at any given time step, we perform first a loop over all particles where individuals move some distance, in a random direction, chosen from a Gaussian distribution of standard deviation  $\sigma$ . At the end of this loop, a second one starts, where (1) each individual with strategy  $x$  dies with a probability obtained from Eq. (2) and (2) if the individual survives the death selection process, it reproduces and the newborn maintains the same location as the parent.

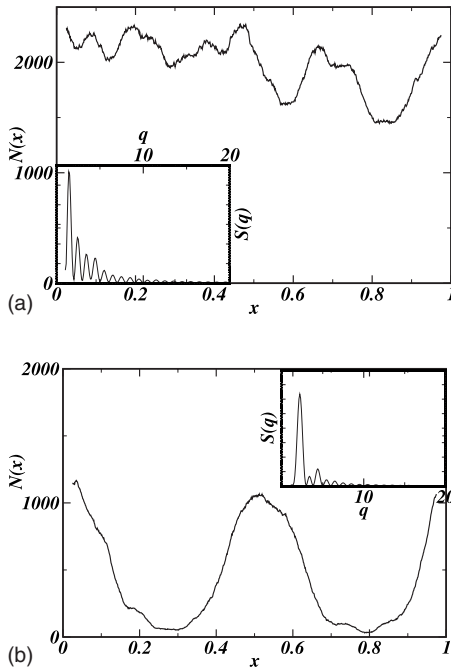


FIG. 1. Homogeneous (top,  $C=4.0$ ,  $1/K=80\,000$ ,  $\sigma=0.01$ ) and modulated (bottom,  $C=0.9$ ,  $1/K=18\,000$ ,  $\sigma=0.01$ ) steady state distributions. The insets show the structure functions  $S(q)$  of the corresponding simulations. We show the distributions at time step 1000, whereas the structure functions are averaged over 500 time steps.

If, in Eq. (1), we measure time in units of the simulation time step, the coefficient  $D$  is related to our simulation parameter through  $D \propto \sigma^2$ . The influence function is given by a Gaussian of standard deviation  $C$  and the effective growth rate is  $1-P$ , with  $P$  given by Eq. (2). This nonconstant growth rate can be represented by Eq. (1) for  $a=1$  and the frequency-dependent part included in the integral term (see Ref. [14]).

Essentially, the only difference between these two versions of our model is that, in the first one, individuals move only at birth, while in the second version they can move at every time step throughout their life. Since the death probability, at equilibrium, is approximately  $1/2$ , usually, in the second version, an individual will move between one and two times during its entire life. For this reason, there should be no relevant differences in the qualitative behavior of the two model implementations. As shown by the measures reported in Sec. IV, the only significant effect is the appearance of slightly wider distributions.

### III. MODULATION

In the following we present some typical examples of steady states generated by the dynamics of the model that clearly show the emergence of patterns for some specific values of the parameters.

For a global competition that is extremely long ranged (large  $C$  values, in relation to the values of parameters  $\sigma$  and  $K$ ), the steady state is characterized by a spatially homoge-

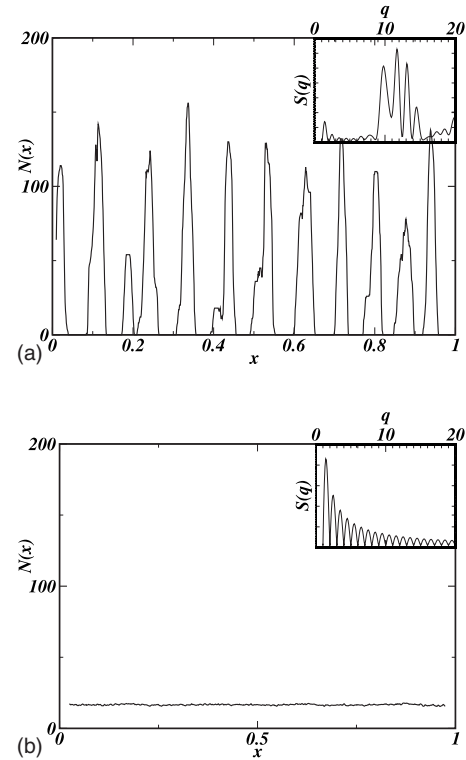


FIG. 2. Spiky (top,  $C=0.059$ ,  $1/K=500$ ,  $\sigma=0.001$ ) and homogeneous (bottom,  $C=0.005$ ,  $1/K=500$ ,  $\sigma=0.001$ ) steady states. The insets show the structure functions  $S(q)$ . We show the distributions at time step 2000, whereas the structure functions are averaged over 1000 time steps. The transition between these two states, in this typical range of parameters, has been extensively studied.

neous occupancy. If the  $\sigma$  value is sufficiently large or/and the  $K$  value sufficiently small, totally homogeneous distributions are obtained (Fig. 1), otherwise the solution is smooth but with the population concentrated in one region of the ring, with its width controlled by  $\sigma$ .

As stated above, a simple heuristic analysis of Eq. (1) in the Fourier space shows that there is a necessary condition for the emergence of inhomogeneity: the Fourier transform of the influence function must have negative values and large enough magnitude [12,13]. A Gaussian in an infinite domain has a positive counterpart in Fourier space and so does not match such requirements. In contrast with these results, the fluctuations present in our individual-based model excite one specific mode, and modulations of this wavelength appear. The tuning of the parameters allows modulations of arbitrary wavelengths (Fig. 1).

When  $C$  is decreased, the competition between modes becomes stronger and no single mode dominates. In this situation, some small regions of the ring are occupied, forcing all the remaining areas, up to some range, to be nearly empty. The landscape becomes populated by several living colonies divided by dead regions. There is almost no competition between individuals of different colonies and the space separating them can be identified with an effective interaction length. This steady state (*spiky state* [10]) corresponds to a sequence of isolated colonies (spikes) and, seen in the Fourier space, many active wavelengths contribute to it (Fig. 2).

Finally, for extremely short-ranged competition, in relation to the  $\sigma$  value, no collective cooperation between different excited modes emerges and a noisy spatially homogeneous distribution appears (Fig. 2).

We describe these paradigmatic steady states of the system by characterizing the related spatial structure with the help of a *structure function*  $S(q)$  [14] defined as follows:

$$S(q) = \left\langle \left| \frac{1}{N(t)} \sum_{j=1}^{N(t)} \exp[i2\pi qx_j(\tau)] \right|^2 \right\rangle_T, \quad (3)$$

where the sum is performed over all individuals  $j$  with their positions determined by  $x_j(\tau)$ . Note that, for convenience, the structure function is calculated only over the closed interval  $[0, L]$ . The function is averaged over some time interval  $T$  in order to avoid noisy data.  $S(0)$  corresponds to the square of the mean number of individuals in the system. The maxima of  $S(q)$  identify the relevant periodicity present in the steady state. We will see that the position of the global maximum ( $q_M$ ) provides an appropriate order parameter for the identification of the segregation transition.

In our study we explored two different initial conditions (ICs). In the first (local ICs), the colony is located in a finite and compact region of the space. In the second (global ICs), the individuals are spread all over the space. The final distribution is independent of this choice and, generally, local initial conditions make the system reach the steady state more slowly. For this reason, if not differently specified, our results are obtained from global initial conditions.

#### IV. FINITE-SIZE EFFECTS

Our analysis starts by exploring the model dependence on the space size  $L$ . The reason for such interest is given by the necessity of testing whether the pattern formation is not merely a product of some finite-size effect. This is important, in the light of what was reported by Fuentes *et al.* in Ref. [12]. In their work, a numerical solution of Eq. (1) with a Gaussian influence function showed a segregation transition. But this transition was just the effect of the finite domain size, which acted like a cutoff for the Gaussian. Evidence of this interpretation came from the observation that the amplitude of the pattern depended on the ratio of the standard deviation of the influence function to the domain size—the critical values of the standard deviation corresponding to the segregation transition depended linearly on the domain size—and the same patterns appeared for a modified Gaussian, which vanishes abruptly beyond a cutoff.

The study of our individual-based model gave different results. By running some simulations with exactly the same parameters but changing the ring extension, we were able to show that the system is not influenced by the domain size. If we choose data from spiky steady states, which permit clear quantitative measures, it is possible to remark that the general morphology of the patterns does not change on increasing the  $L$  value. In fact, both the population density and the mean number of peaks per space interval remain constant. Moreover, in order to provide a more precise test of possible small variations in the distribution, we measured the cluster

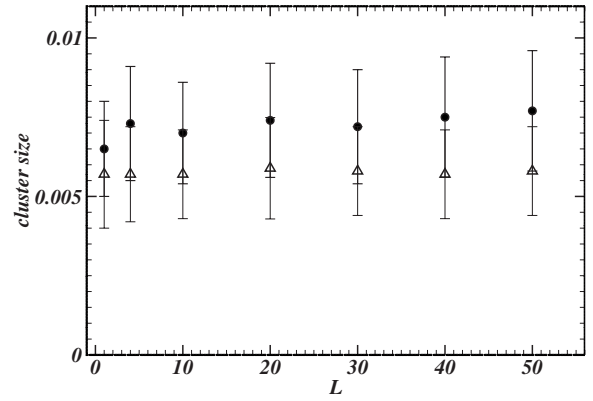


FIG. 3. Dependence of the cluster size on the ring size  $L$ . We present data from the model with mutation (triangles) and from the one that implements diffusion (circles).  $C=0.2$ ,  $K=0.0029$ ,  $\sigma=0.001$ . The average is carried out over all the clusters present at a given time step and over different time steps.

size. This quantity was calculated by evaluating the standard deviation  $(\langle x^2 \rangle_i - \langle x \rangle_i^2)^{1/2}$  of the position of the  $i$  individuals confined in each peak, then averaged over the different peaks present at step  $\tau$ , and, finally, averaged over many time steps after the system has reached the steady state.

Varying the system size caused no changes in the clusters size (see Fig. 3). From this result, we concluded that the general aspect of the steady state does not change with  $L$ . In particular, in contrast with what happens when the mean-field equation is solved numerically, the patterns do not depend on the ratio  $C/L$ . For example, for  $C=0.2$  and  $L=50$  we obtained a spiky steady state; for  $C=0.004$  and  $L=1$  (same ratio) we obtained a homogeneous steady state. Taking into account these results, from now on, all our simulations are implemented on a ring of size 1.

We have just shown how the average of the population size  $\langle N \rangle$  scales with  $L$  in the steady state. Now, we will give, through a simple heuristic argument, an estimation of  $\langle N \rangle$  as a function of the parameters  $K$  and  $C$ , which will be useful also in the rest of our analysis.

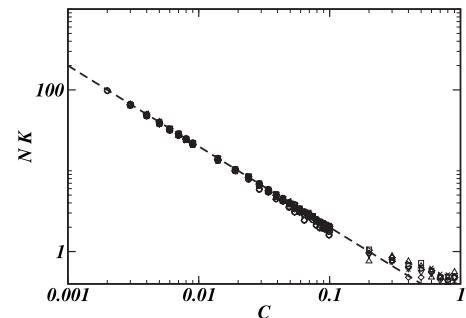


FIG. 4. The number of individuals  $N$  present in the steady state is proportional to  $(CK)^{-1}$ . This result is in accordance with the one obtained for a box-type influence function of length  $C$  (see Ref. [32]). We present data for different simulations with  $1/K \in [50, 500]$  and  $\sigma \in [0.0001, 0.01]$ . This last parameter does not influence the final number of individuals. The dashed line has slope  $-1$ .

We can assume that, locally and in the steady state, the number of deaths must be, on average, compensated by the number of newborns, in order to comprise a stable population. For this reason, the death probability  $P$  must equal  $1/2$ . Assuming that the number of neighbors that compete with a single individual are the ones living up to a distance  $C$  and that, in these surroundings, the average density  $N/L$  can be considered to be uniform,  $P$  reduces to  $K \times 2C \times N/L$ . Thus,  $N \propto L/(CK)$ . Looking at Fig. 4, we can see that this crude evaluation, which neglects diffusion and inhomogeneity and reduces the influence function to a box, describes well the general behavior of the data obtained from our simulations.

**V. SEGREGATION TRANSITION**

In the previous sections, we supported the fact that steady states, depending on the parameter values, can assume inhomogeneous spatial distributions. Now, we will try to describe the transition toward these states (segregation transition). The structure function introduced in Eq. (3) provides a proper order parameter to describe this transition. Different regions in the parameter space, coinciding with different steady states, correspond to different positions of the global maximum [obviously we are not taking into account  $S(q)$  at  $q=0$ ] of the structure function. The transition from a homogeneous to an inhomogeneous distribution (see Fig. 2) matches the jump of the position of the global maximum ( $q_M$ ) to a clear integer value, corresponding to the number of clusters present in the space. For this reason we can charac-

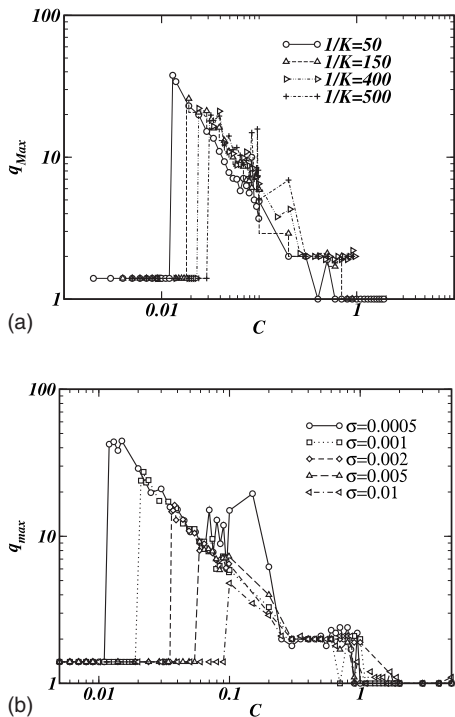


FIG. 5. Segregation transition at  $C_{crit}$ . Upper figure: variation in dependence on  $K$ , where  $1/K=50, 150, 400, 500$ , and  $\sigma=0.001$ . Lower figure: variation in dependence on  $\sigma$ , where  $\sigma=0.0005, 0.001, 0.002, 0.005, 0.01$ , and  $1/K=200$ .

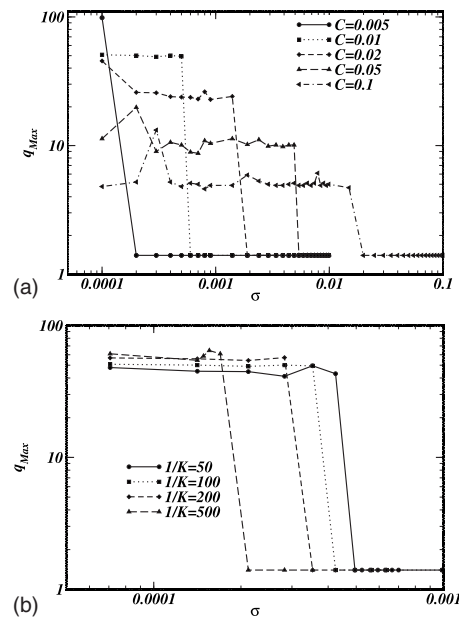


FIG. 6. Showing the existence of a critical  $\sigma$  value above which no spatial structures emerge. Upper figure: variation in dependence on  $C$ ; we set  $1/K=100$ . Lower figure: variation in dependence on  $K$ ; we set  $C=0.01$ .

terize the transition by looking at the shape assumed by  $S(q)$ , or looking at the value of  $q_M$ . If the space is homogeneously occupied, the structure function does not present an integer maximum. On the contrary, the maximum is located at  $q_M \approx 1.4$ . This value corresponds to a uniform distribution of individuals in the interval  $[0,1]$ , approximated by the expression  $|\int_0^1 \exp(i2\pi qx) dx|^2$ . The segregation transition is characterized by the passage of  $q_M$  from 1.4 to an integer value as soon as a modulation becomes dominant. In Fig. 5 we show  $q_M$  as a function of  $C$ , varying  $K$  and  $\sigma$ . First of all, from the analysis of these data, we can observe that the number of clusters scales as  $C^{-1}$  (or, equivalently, the periodicity of the inhomogeneous phase has wavelengths proportional to  $C$ ). Moreover, a critical value of  $C$  exists for which the transition takes place. This  $C_{crit}$  grows with  $1/K$  and with  $\sigma$ . An analysis of the available data suggests the possible dependence:  $C_{crit} \propto \sigma^{2/3} K^{-1/3}$ . Finally, for larger values of the parameter  $C$ , in this range of the parameters  $\sigma$  and  $K$ , the distributions are characterized by just one peak.

For any value of the competition strength, as can be seen in Fig. 6, there exists a critical value  $\sigma_{crit}$ , dependent on  $C$  and  $K$ , above which no spatial structures emerge. Another measurement, which permits us to state this relation in a different and clearer way, is presented in the next section.

**VI. CLUSTER SIZE AND FLUCTUATIONS**

In the following we describe, in the light of the existing literature, the cluster size dependence on diffusion rate and population size for the two different implementations of the model.

We start by analyzing the typical size  $S$  of the clusters that appear in the spiky phase. The data in Fig. 7 show a depen-

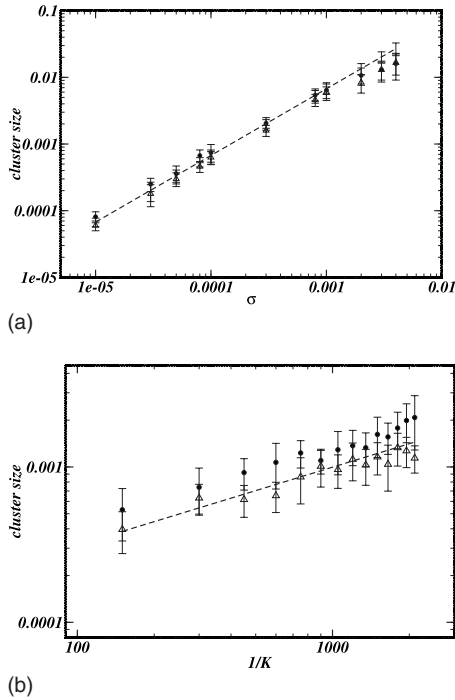


FIG. 7. Top: Cluster size as a function of  $\sigma$ ;  $1/K=300$ . The solid line has slope 1. Bottom: Cluster size as a function of  $1/K$ ;  $\sigma=0.0001$ . The solid line has slope  $1/2$ . Triangles represent data from the simulations where diffusion is implemented through mutations, circles for the direct implementation of the diffusive process; we set  $C=0.09$ .

dence of the cluster size on the diffusion coefficient  $S \propto \sigma$ , equivalent to  $S \propto \sqrt{D}$ . These results are in accordance with the data presented in Ref. [33], obtained from an individual-based model. In addition, this work pointed out how this behavior deviates from the conclusions obtained from the deterministic approximation, where the cluster size was only weakly dependent on the diffusion coefficient, another fact supporting the relevance of fluctuation effects in these systems.

We can easily interpret the dependence of the cluster size on the diffusion coefficient by assuming that the individuals confined in a cluster diffuse a distance proportional to  $\sqrt{DJ}$ , where  $J$  is the number of jumps the individual performs in its life. In the case of the first implementation of the model, where the diffusion is due to the mutation process,  $J$  is obviously 1. Similar results are obtained with the second implementation (see Fig. 7), apart from a slightly wider cluster size (in this case, individuals move, on average, more than just once during their lifetime). Even so, the data show the same dependence on the diffusion coefficient.

Finally, we present  $S$  as a function of  $K$ :  $S \propto \sqrt{1/K}$ . The reasons for this behavior are already explained in Ref. [34]: the cluster size is not controlled just by the single individual's number of jumps; in fact, the diffusive process continues with its descendants. For this reason, it is proportional to the mean lifetime of a family, estimated to be proportional to  $K^{-1}$  (see Ref. [34] for details).

We introduce a quantity that is useful for describing the existence of a critical diffusion value, giving an estimation of

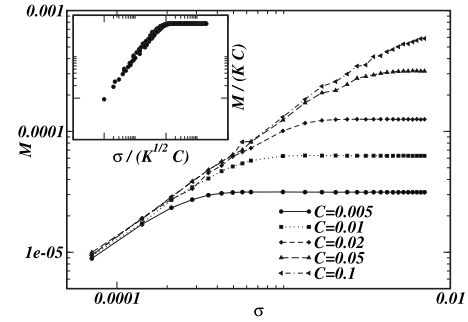


FIG. 8. Mobility dependence on the diffusion parameter  $\sigma$  for different  $C$  values;  $K=0.01$ . In the inset, the data collapse for arbitrary values of the parameters  $C$  and  $K$ .

its dependence on other parameters and a confirmation of previous results. This quantity, which we call the *mobility*  $M(\tau)$ , estimates the mean mobility of individuals. At a given time step  $\tau$ , we choose an individual  $i$ . Then we look for the closest agent, among all the population, at time step  $\tau-1$ . We identify as  $d_i$  the distance between these two individuals. Averaging over the entire population  $N(\tau)$ , we obtain

$$M(\tau) = \frac{1}{N(\tau)} \sum_{i=1}^{N(\tau)} d_i. \quad (4)$$

The values assumed by  $M$  on varying the parameters  $\sigma$  and  $C$  are shown in Fig. 8. It is easy to distinguish two clearly different behaviors. If the system is organized in a spiky state (when  $\sigma \leq \sigma_{\text{crit}}$ ),  $M(\tau) \propto \sigma$ .  $M$  is another way of measuring the mean distance that an individual moves during its lifetime inside the region defined by the cluster. For this reason, this measure is coherent with the data obtained from the direct evaluation of the standard deviation of the clusters. In contrast, when the system is organized in the homogeneous phase (when  $\sigma > \sigma_{\text{crit}}$ )  $M$  becomes independent of  $\sigma$  and is proportional to the inverse of the occupation density  $M(\tau) \propto KC$ . The values of the mobility obtained from simulations with different values of  $C$  and  $K$  can be easily collapsed into one function (see the inset of Fig. 8). The collapse is performed using the scaling  $\sigma \rightarrow \sigma/C\sqrt{K}$ . This indicates that the characteristic value of the crossover,  $\sigma_{\text{crit}}$ , that separates the two different behaviors of  $M(\tau)$  scales as

$$\sigma_{\text{crit}} \propto C\sqrt{K}. \quad (5)$$

We conclude our study with some measurements trying to catch some properties of the system fluctuations. First, we estimated the fluctuations of the total population, averaging over different simulations. The variance turned out to be constant throughout the time evolution and of the order of the square root of the total population. The mechanism of auto-regulation of the population dimension does not allow the growth of big differences in the total number of individuals.

For this reason, we focused our attention on the spatial distribution of the population and tried to measure some properties of these fluctuations. We studied the variation of the local number of individuals in the same simulation, for different times. We analyzed the evolution of the system

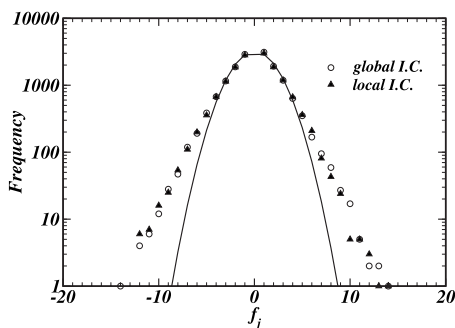


FIG. 9. Spatial local fluctuation distribution at the steady state: deviation from a Gaussian ( $C=0.1$ ,  $K=0.000\ 05$ ,  $\sigma=0.0017$ ). Data are averaged over 5 time steps. The continuous line is the best-fit Gaussian.

starting from local initial conditions, with the population concentrated in the interval  $[0.49, 0.51]$ . In this situation, the system evolves in time with a small cluster fluctuating around the initial space interval. This situation changes when a branching event occurs that generates two well-defined clusters. Our interest is in showing the behavior of local space fluctuations and capturing possible variations in correspondence with the branching event. First of all, we looked at the mean value of the spatial local fluctuations  $F_s(\tau)$ , defined as  $F_s(\tau) = (\sum_{j=1}^b f_j^2)^{1/2}$ , where  $f_j$  is the occupancy variation of the bin  $j$  from time step  $\tau-1$  to time step  $\tau$ . We performed the average over all  $b$  bins in the ring and obtained  $F_s(\tau) = \sqrt{N(\tau)}$ , with no relevant variations throughout the time evolution, even in the time interval corresponding to the branching event. More interesting is the shape of the frequency distribution of the size of  $f_j$ . In fact, a simple Gaussian does not fit this distribution, which presents extended tails (see Fig. 9). Throughout the system time evolution, the shape of the normalized distribution is conserved. For global initial conditions, the same frequency distribution, with extended tails, is recovered at the steady state. It is identical to the one obtained with local initial conditions and measured at the steady state. We think that the deviation of

the distribution from a Gaussian can be considered as a hint that fluctuations play a relevant role in the dynamics of the systems.

## VII. CONCLUSIONS

We presented some results regarding clustering of organisms caused by a frequency-dependent interaction that represents competition. We showed how this way of modeling competition can be used not only to describe spatial phenomena in population biology, but also, through a more abstract interpretation, to test ideas of evolutionary theory (for example, studying the speciation process).

From this unifying perspective, our study, obtained from an extensive collection of data coming from simulations of an individual-based model with global competition, pointed out the relevance of fluctuation effects in pattern formation. For the influence function adopted, the mean-field description predicts the absence of spatial structures. On the contrary, fluctuations are able to excite the emergence of well-defined patterns, which cannot be generated from a deterministic instability.

Furthermore, we discussed other fundamental properties of our model in the light of the existing literature, unfolding a comparison with other models that describe spatial segregation originated by some deterministic instability. We showed that the observed patterns are not due to a finite-size effect, we characterized the behavior of the segregation transition in various regions of the parameter space, and we studied the existence of a critical diffusion value. We analyzed the dependence of the cluster size on the diffusion coefficient and pointed out some characteristics of the fluctuations of the system.

## ACKNOWLEDGMENT

We are grateful to J. S. Sá Martins for a critical reading of the manuscript and thank the Brazilian agency CNPq for financial support.

- 
- [1] S. A. Levin and L. A. Segel, *SIAM Rev.* **27**, 45 (1985); R. Durrett and S. A. Levin, *Philos. Trans. R. Soc. London, Ser. B* **343**, 329 (1994).
  - [2] Y.-C. Zhang, M. Serva, and M. Polikarpov, *J. Stat. Phys.* **58**, 849 (1990).
  - [3] N. M. Shnerb, Y. Louzoun, E. Bettelheim, and S. Solomon, *Proc. Natl. Acad. Sci. U.S.A.* **97**, 10322 (2000).
  - [4] B. Houchmandzadeh, *Phys. Rev. E* **66**, 052902 (2002).
  - [5] W. R. Young, A. J. Roberts, and G. Stuhne, *Nature (London)* **412**, 328 (2001).
  - [6] E. Ben-Jacob, I. Cohen, and H. Levine, *Adv. Phys.* **49**, 395 (2000); J. Wakita, K. Komatsu, A. Nakahara, T. Matsuyama, and M. Matsushita, *J. Phys. Soc. Jpn.* **63**, 1205 (1994).
  - [7] K. S. McCann, J. B. Rasmussen, and J. Umbanhowar, *Ecol. Lett.* **8**, 513 (2005).
  - [8] J. B. Wilson and A. D. Q. Agnew, *Adv. Ecol. Res.* **23**, 263 (1992); R. Lefever and O. Lejeune, *Bull. Math. Biol.* **59**, 263 (1997); N. M. Shnerb, P. Sarah, H. Lavee, and S. Solomon, *Phys. Rev. Lett.* **90**, 038101 (2003).
  - [9] N. F. Britton, *SIAM J. Appl. Math.* **50**, 1663 (1990); S. A. Gourley and N. F. Britton, *J. Math. Biol.* **34**, 297 (1996).
  - [10] Y. E. Maruvka and N. M. Shnerb, *Phys. Rev. E* **73**, 011903 (2006).
  - [11] A. Sasaki, *J. Theor. Biol.* **186**, 415 (1997).
  - [12] M. A. Fuentes, M. N. Kuperman, and V. M. Kenkre, *Phys. Rev. Lett.* **91**, 158104 (2003).
  - [13] M. A. Fuentes, M. N. Kuperman, and V. M. Kenkre, *J. Phys. Chem. B* **108**, 10505 (2004).
  - [14] E. Hernandez-Garcia and C. Lopez, *Phys. Rev. E* **70**, 016216 (2004).

- [15] D. R. Nelson and N. M. Shnerb, *Phys. Rev. E* **58**, 1383 (1998).
- [16] G. Flierl, D. Grunbaum, S. Levin, and D. Olson, *J. Theor. Biol.* **196**, 397 (1999).
- [17] B. M. Bolker, *Theor. Popul. Biol.* **64**, 255 (2003).
- [18] J. Roughgarden, *Am. Nat.* **106**, 683 (1972).
- [19] F. Bagnoli and M. Bezzi, *Phys. Rev. Lett.* **79**, 3302 (1997).
- [20] U. Dieckmann and M. Doebeli, *Nature (London)* **400**, 354 (1999); M. Doebeli and U. Dieckmann, *ibid.* **421**, 259 (2003).
- [21] E. Brigatti, J. S. Sá Martins, and I. Roditi, *Physica A* **376**, 378 (2007); V. Schwämmle and E. Brigatti, *Europhys. Lett.* **75**, 342 (2006).
- [22] S. Pigolotti, C. Lopez, and E. Hernandez-Garcia, *Phys. Rev. Lett.* **98**, 258101 (2007).
- [23] H. Sayama, M. A. M. de Aguiar, Y. Bar-Yam, and M. Baranger, *Phys. Rev. E* **65**, 051919 (2002).
- [24] D. A. Kurtze, *Phys. Rev. B* **40**, 11104 (1989).
- [25] F.-J. Elmer, *Phys. Rev. Lett.* **70**, 2028 (1993).
- [26] J. Billingham, *Nonlinearity* **17**, 313 (2004).
- [27] H. Sayama, L. Kaufman, and Y. Bar-Yam, *Phys. Rev. E* **62**, 7065 (2000).
- [28] R. A. Fisher, *Ann. Eugen.* **7**, 353 (1937); A. Kolmogoroff, I. Petrovsky, and N. Piscounoff, *Moscow Univ. Bull. Math.* **1**, 1 (1937).
- [29] F. J. Weissing and J. Huisman, *J. Theor. Biol.* **168**, 323 (1994).
- [30] J. Polechova and N. H. Barton, *Evolution (Lawrence, Kans.)* **59**, 1194 (2005).
- [31] M. Meyer, S. Havlin, and A. Bunde, *Phys. Rev. E* **54**, 5567 (1996).
- [32] C. Lopez and E. Hernandez-Garcia, *Physica D* **199**, 223 (2004).
- [33] E. Hernandez-Garcia and C. Lopez, *Physica A* **356**, 95 (2005).
- [34] E. Hernandez-Garcia and C. Lopez, *J. Phys.: Condens. Matter* **17**, S4263 (2005).